

# Step, Ramp, Delta, and Differentiable Activation Functions Obtained Using Percolation Equations

David S. McLachlan<sup>1,\*</sup>, Godfrey Sauti<sup>2</sup>

<sup>1</sup>School of Physics, University of the Witwatersrand, Johannesburg 2050, South Africa

<sup>2</sup>Advanced Materials and Processing Branch, NASA Langley Research Center, United States

Received June 12, 2022; Revised September 29, 2022; Accepted October 11, 2022

Cite This Paper in the following Citation Styles

(a): [1] David S. McLachlan, Godfrey Sauti, "Step, Ramp, Delta, and Differentiable Activation Functions Obtained Using Percolation Equations," *Mathematics and Statistics*, Vol.10, No.6, pp. 1206-1209, 2022. DOI: 10.13189/ms.2022.100606

(b): David S. McLachlan, Godfrey Sauti (2022). *Step, Ramp, Delta, and Differentiable Activation Functions Obtained Using Percolation Equations*. *Mathematics and Statistics*, 10(6), 1206-1209. DOI: 10.13189/ms.2022.100606

Copyright ©2022 by authors, all rights reserved. Authors agree that this article remains permanently open access under the terms of the Creative Commons Attribution License 4.0 International License

**Abstract** This paper presents two new analytical equations, the Two Exponent Phenomenological Percolation Equation (TEPPE) and the Single Exponent Phenomenological Percolation Equation (SEPPE) which, for the proper choice of parameters, approximate the widely used Heaviside Step Function. The plots of the equations presented in the figures in this paper show some, but by no means all, of the step, ramp, delta, and differentiable activation functions that can be obtained using the percolation equations. By adjusting the parameters these equations can give linear, concave, and convex ramp functions, which are basic signals in systems used in engineering and management. The equations are also Analytic Activation Functions, the form or nature of which can be varied by changing the parameters. Differentiating these functions gives delta functions, the height and width of which depend on the parameters used.

The TEPPE and SEPPE and their derivatives are presented in terms of the conductivity ( $\sigma$ ) owing to their original use in describing the electrical properties of binary composites, but are applicable to other percolative phenomena. The plots in the figures presented are used to show the response  $\sigma_m$  (composite conductivity) for the parameters  $\sigma_h$  (higher conductivity component of the composite),  $\sigma_l$  (lower conductivity component of the composite) and  $\phi$ , the volume fraction of the higher conductivity component in the composite. The additional parameters are the critical volume fraction,  $\phi_c$ , which determines the position of the step or delta function on the  $\phi$  ( $0 - 1$ ) axis and one or two exponents  $s$ , and  $t$ .

**Keywords** Percolation, Step Functions, Delta Functions, Activation Functions, Neural Networks

## 1 Introduction and Theory

In this paper, it will be shown that sigmoidal, step, linear, convex and concave ramp functions, narrow delta (impulse) functions and differentiable activation functions can be obtained from the Single Exponent Phenomenological Percolation Equation (SEPPE) or the Two Exponent Phenomenological Percolation Equation (TEPPE). The paper will begin by presenting these two equations [1, 2]. The SEPPE and TEPPE equations are written as they would be used to model the electrical conductivity,  $\sigma_m$ , of a binary composite, as it is in this field that they have been most widely used. The equation for ( $\sigma_m$ ), contains the following components or parameters, a high conductivity component ( $\sigma_h$ ) and a low conductivity component ( $\sigma_l$ ), and is a function of the volume fraction ( $\phi$ ) of the high conductivity component. The other parameters are the critical volume fraction ( $\phi_c$ ) and the percolation exponents  $s$ , and  $t$ . Physically,  $\phi_c$  is where the high conductivity component ( $\sigma_h$ ) first forms a continuous path through the composite. Mathematically,  $\phi_c$ , which lies between 0 and 1, is the position of the steepest slope of the resulting sigmoidal (step) function or the peak of a delta function and can lie anywhere between 0 and 1. In the mathematical usage of these equations  $\sigma_m$ ,  $\sigma_h$ ,  $\sigma_l$ ,  $\phi_c$ ,  $s$ , and  $t$  are dimensionless.

The TEPPE is:

$$(1 - \phi) \frac{\sigma_l^{\frac{1}{s}} - \sigma_m^{\frac{1}{s}}}{\sigma_l^{\frac{1}{s}} + A\sigma_m^{\frac{1}{s}}} + \phi \frac{\sigma_h^{\frac{1}{t}} - \sigma_m^{\frac{1}{t}}}{\sigma_h^{\frac{1}{t}} + A\sigma_m^{\frac{1}{t}}} = 0 \quad (1)$$

Here  $A = (1 - \phi_c)/\phi_c$  and an equation for  $\sigma_m$  is obtained

by solving Eq. 1. The SEPPE is obtained by putting  $s = t$ . These equations [1, 2] are a phenomenological parameterization of the Bruggeman Symmetric Media Equation [1], which was analytically derived from first principles. The TEPPE reduces to the three original percolation equations [3, 4] in the correct limits (see below).

The results given here and most experimental results, are usually presented as plots of  $\log \sigma_m(\phi)$  against  $\phi$ , which give characteristic sigmoidal plots, for sufficiently high values of  $\sigma_h/\sigma_l$ . The point of inflection, or in the extreme case a step, in these curves occurs at  $\phi_c$ . The plots presented here are obtained from the much simpler and tractable SEPPE. The TEPPE allows one to independently adjust the curvature of plot of  $\log \sigma_m(\phi)$  against  $\phi$ , on either side of  $\phi_c$ .

Equation 1, with independent  $s$  and  $t$ , yields two limits:

$$\sigma_h \rightarrow \infty : \quad \sigma_m = \sigma_l \left( \frac{\phi_c}{\phi_c - \phi} \right)^s, \quad \phi < \phi_c \leq 1 \quad (2a)$$

$$\sigma_l \rightarrow 0 : \quad \sigma_m = \sigma_h \left( \frac{\phi_c}{1 - \phi_c} \right)^t, \quad \phi > \phi_c \geq 0 \quad (2b)$$

These equations show that the normalized percolation equations [3, 4] are special cases of the TEPPE, when  $\phi$  approaches 1 or 0. These equations define the exponents  $s$  and  $t$ . The region close to  $\phi_c$  where both components play a major role in determining the conductivity, is called the cross-over region [3, 4].

Unlike the original percolation equations [3, 4] the SEPPE and TEPPE are valid for all  $\phi$  between 0 and 1, including the cross-over region.

In this paper, the delta functions are obtained from the equation

$$\Delta = \frac{1}{\sigma_m(\phi)} \frac{d\sigma_m(\phi)}{d\phi} \quad (3)$$

The equations given in this paper are not the only analytic expressions used to obtain approximations to the Heaviside step function. There are several of such expressions given in Wikipedia: Heaviside step function [5]. These all make use of either the tanh, the arctan or erf functions, all of which include the exponential function. More recent advances in this field as well as two new analytic approximations of the Heaviside function can be found in [6, 7].

It is not claimed that the SEPPE or TEPPE is superior to any or all of the existing analytic functions. However, it may well be that in some applications they may prove to be a better choice. Note that these are the only analytic step functions that are based on power laws and in which the position of the step or delta function can be controlled by a single parameter.

## 2 Experimental Results

Experimental results which have been analysed using either the SEPPE or TEPPE can be found in references [1, 2, 8, 9, 10, 11, 12, 13]. These experimental results include work on electrical and thermal conductivity, permeability and permittivity

of binary composites or systems where there are two highly insulating components, one of which is usually air or vacuum. These results are evaluated treating  $\sigma_l$  as a single component which is then a weighted average of the two insulating components. One preliminary set of results on an air-sintered nickel system shows that the Young's modulus can also be modeled using the SEPPE [8]. Results have been obtained from both static and dynamic measurements. In the latter case the relevant parameters for the composite and the two components are complex valued quantities. An analysis of systems of magnetic granular composites is found in [9]. A qualitative discussion of various models for  $\phi_c$  is given in [8].

Experimental results give  $s$  in the range from about 1 to as low as 0.4 [13]. Experimental  $t$  values span a large range and can depend on whether the electrical conductivity, the thermal conductivity or permeability is being measured [13]. Some of the results are not fully understood. For instance, a non-hysteretic Gadolinium Gallium Garnet-Teflon system (measured at 2 K), a  $\text{Fe}_3\text{O}_4$ -talc wax system and a Ni-talc wax system [11] give  $t$  values of about 4 for conductivity measurements, but  $t$  values in the range of 0.4 to 0.5 from permeability measurements [13]. As this is primarily a mathematical paper, further experimental details will not be given here.

## 3 Step and Ramp Functions

The plots given in this paper are selected to illustrate the potential of the functions discussed and are by no means exhaustive. Shown in Fig. 1 are plots of  $\log \sigma_m(\phi)$  of the SEPPE with  $\sigma_l = 10^{-6}$  and  $\sigma_h = 10^6$ ,  $A = 1(\phi_c = 0.5)$  and  $t$  values between 0.01 and 2. Shown in Fig. 2 are plots of the same results on a linear scale where the  $\sigma_m$  results have been normalized by  $\sigma_h = 10^6$ . Very sharp step functions, shown in Fig. 2, can be obtained for low values of  $t$ . The "sharpness" of the step function must be gauged from the derivatives given in Section 4. Note that the plot for  $t = 1.0$ , in Fig. 2 is a linear ramp function. Convex ramp functions are obtained for  $t > 1$  and concave ramp functions for  $t < 1$ .

Using the TEPPE enables the curvature on both sides of  $\phi_c$  to be individually varied.

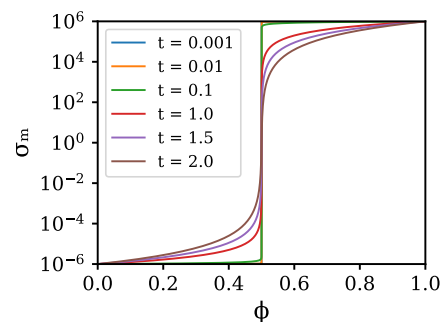


**Figure 1.** Log-linear plots of  $\sigma_m(\phi)$  of the SEPPE with  $\sigma_l = 10^{-6}$  and  $\sigma_h = 10^6$ ,  $A = 1(\phi_c = 0.5)$  and  $t$  values between 0.001 and 2.

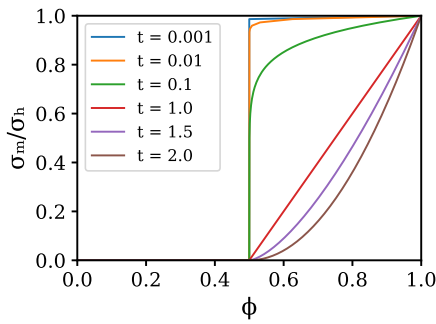


**Figure 2.** Normalized linear plots of  $\sigma_m(\phi)/\sigma_h$  of the SEPPE with  $\sigma_l = 10^{-6}$  and  $\sigma_h = 10^6$ ,  $A = 1(\phi_c = 0.5)$  and  $t$  values between 0.001 and 2.

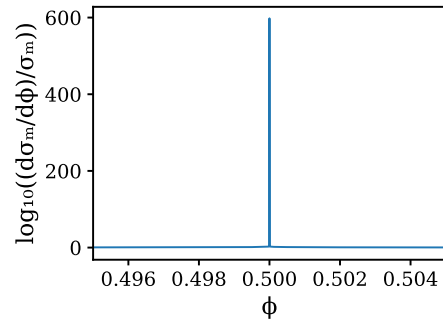


**Figure 4.** A plot of  $\log(1/\sigma_m(\phi)d\sigma_m(\phi)/d\phi)/\sigma_m$  against  $\phi$  (between 0.495 and 0.505) with  $\sigma_l = 10^{-6}$  and  $\sigma_h = 10^6$ , and  $A = 1(\phi_c = 0.5)$  with  $t = 0.01$ .

### 4 Activation Functions

In Fig. 3, the SEPPE is plotted on a linear 0 to 1 scale, with  $\sigma_l = 0.01$  and  $\sigma_h = 1$ ,  $A = 1(\phi_c = 0.5)$  and  $t$  values between 0.001 and 2. The illustrative plots shown in Fig. 3 indicate that the SEPPE (and TEPPE) can, for different values of  $\sigma_l$ ,  $\sigma_h$  and  $t$ , be used to generate a variety of differentiable activation functions. When  $t$  is very low (0.001 or lower), the function approximates a Binary Step Activation Function [14, 15].

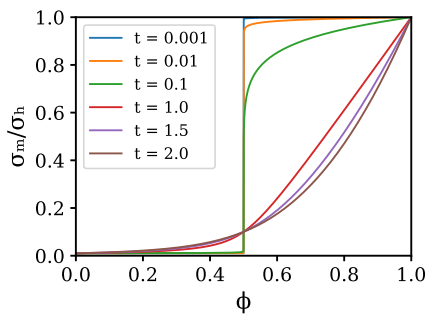


**Figure 3.** Plot of  $(\sigma_m(\phi))/\sigma_h$  of the SEPPE with  $\sigma_l = 0.01$  and  $\sigma_h = 1.0$ ,  $A = 1(\phi_c = 0.5)$  and  $t$  values between 0.001 and 2.

Examples are given in [14, 15] of both sigmoidal and tanh activation functions. Tanh type activation functions can be obtained by subtracting  $\sigma_h/2$  from Eq. 1 which results in a tanh type function with  $\sigma_m = -\sigma_h/2$  at  $\phi = 0$  and  $\sigma_m = \sigma_h/2$  at  $\phi = 1$ .

### 5 Delta Functions

Various delta functions obtained from Eq. 3 are shown in Figs. 4 to 7. Plots are shown in Figs. 4 and 5 of  $\log(1/\sigma_m(\phi)d\sigma_m(\phi)/d\phi)$  against  $\phi$  (between 0.495 and 0.505) with  $\sigma_l = 10^{-6}$  and  $\sigma_h = 10^6$ , and  $A = 1(\phi_c = 0.5)$  with  $t = 0.01$  and 0.1 respectively. The narrow width of these delta functions is very apparent. Plots are shown in Figs. 6 and 7 of  $\log(1/\sigma_m(\phi)d\sigma_m(\phi)/d\phi)$  against  $\phi$  (between 0 and 1) with  $\sigma_l = 10^{-6}$  and  $\sigma_h = 10^6$ , and  $A = 1(\phi_c = 0.5)$  with  $t = 1$  and 2 respectively. The shape of the spikes is illustrated in the plots.

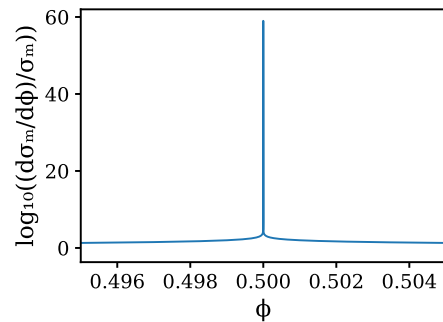


**Figure 5.** A plot of  $\log(1/\sigma_m(\phi)d\sigma_m(\phi)/d\phi)/\sigma_m$  against  $\phi$  (between 0.495 and 0.505) with  $\sigma_l = 10^{-6}$  and  $\sigma_h = 10^6$ , and  $A = 1(\phi_c = 0.5)$  with  $t = 0.1$ .

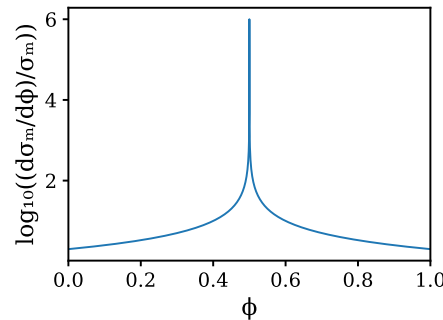


**Figure 6.** A plot of  $\log(1/\sigma_m(\phi)d\sigma_m(\phi)/d\phi)/\sigma_m$  against  $\phi$  (between 0 and 1) with  $\sigma_l = 10^{-6}$  and  $\sigma_h = 10^6$ , and  $A = 1(\phi_c = 0.5)$  with  $t = 1$ .

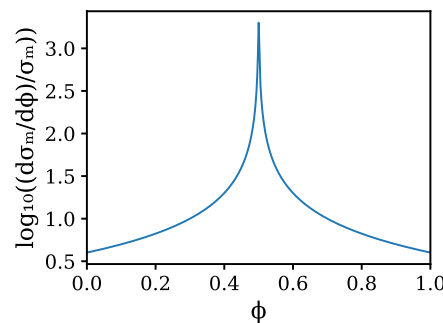


**Figure 7.** A plot of  $\log(1/\sigma_m(\phi)d\sigma_m(\phi)/d\phi)/\sigma_m$  against  $\phi$  (between 0 and 1) with  $\sigma_l = 10^{-6}$  and  $\sigma_h = 10^6$ , and  $A = 1(\phi_c = 0.5)$  with  $t = 2$ .

## 6 Conclusions

The SEPPE, which is widely used to model the transport properties of binary composites, gives sigmoidal step, linear, convex, and concave ramp functions and differentiable sigmoidal and tanh type activation functions. Extensions to the SEPPE using the TEPPE are also mentioned.

In Eq. 1 in this paper, the position of the step, ramp or delta function is controlled by a single parameter  $\phi_c$ . In the case of the SEPPE, the shape of the function is largely determined by the exponent  $t$ . In the case of the TEPPE, the shape is controlled by both the exponents  $s$  and  $t$ . The functions given in this paper can be used to generate plots very similar to some of the different types of Neural Network Activation functions curves given in [14, 15]. It must be noted that the functions given in [14, 15] are functions of a variable  $x$ , which goes from  $-X$  to  $+X$ . The steps or deltas of these functions always occur at  $x = 0$ .

## REFERENCES

- [1] D. S. McLachlan, M. Blaszkiewicz, and R. E. Newnham, "Electrical resistivity of composites," *Journal of the American Ceramic Society*, vol. 73, no. 8, pp. 2187–2203, 1990. [Online]. Available: <https://ceramics.onlinelibrary.wiley.com/doi/abs/10.1111/j.1151-2916.1990.tb07576.x>
- [2] J. Wu and D. S. McLachlan, "Percolation exponents and thresholds obtained from the nearly ideal continuum percolation system graphite-boron nitride," *Phys. Rev. B*, vol. 56, pp. 1236–1248, Jul 1997. [Online]. Available: <https://link.aps.org/doi/10.1103/PhysRevB.56.1236>
- [3] J. Clerc, G. Giraud, J. Laugier, and J. Luck, "The electrical conductivity of binary disordered systems, percolation clusters, fractals and related models," *Advances in Physics*, vol. 39, no. 3, pp. 191–309, 1990. [Online]. Available: <https://doi.org/10.1080/00018739000101501>
- [4] D. J. Bergman and D. Stroud, "Physical properties of macroscopically inhomogeneous media," ser. Solid State Physics, H. Ehrenreich and D. Turnbull, Eds. Academic Press, 1992, vol. 46, pp. 147–269. [Online]. Available: <https://www.sciencedirect.com/science/article/pii/S0081194708603987>
- [5] Wikipedia contributors, "Heaviside step function — Wikipedia, the free encyclopedia," 2022, [Online; accessed 25-April-2022]. [Online]. Available: [https://en.wikipedia.org/w/index.php?title=Heaviside\\_step\\_function&oldid=1081077108](https://en.wikipedia.org/w/index.php?title=Heaviside_step_function&oldid=1081077108)
- [6] J. Venetis, "An analytic exact form of the unit step function," *Mathematics and Statistics*, DOI: 10.13189/ms.2014.020702, vol. 2, pp. 235 – 237, 10 2014.
- [7] —, "Analytic exact forms of heaviside and dirac delta function," *Advances in Dynamical Systems and Applications*, vol. 15, pp. 115–121, 09 2020.
- [8] D. S. McLachlan, "Analytical functions for the dc and ac conductivity of conductor-insulator composites," *Journal of Electroceramics*, vol. 5, no. 2, pp. 93–110, Oct 2000. [Online]. Available: <https://doi.org/10.1023/A:1009954017351>
- [9] P. Chen, R. X. Wu, T. Zhao, F. Yang, and J. Q. Xiao, "Complex permittivity and permeability of metallic magnetic granular composites at microwave frequencies," *Journal of Physics D: Applied Physics*, vol. 38, no. 14, pp. 2302–2305, jul 2005. [Online]. Available: <https://doi.org/10.1088/0022-3727/38/14/002>
- [10] D. S. McLachlan and G. Sauti, "The ac and dc conductivity of nanocomposites," *Journal of Nanomaterials*, vol. 2007, p. 030389, Nov 2007. [Online]. Available: <https://doi.org/10.1155/2007/30389>
- [11] D. S. McLachlan, T. B. Doyle, and G. Sauti, "Percolation behaviour in the magnetic permeability and electrical conductivity in conducting magnetic – insulating non magnetic binary composites," *Journal of Magnetism and Magnetic Materials*, vol. 458, pp. 365–370, 2018. [Online]. Available: <https://www.sciencedirect.com/science/article/pii/S0304885317337460>
- [12] B. Ghanbarian and H. Daigle, "Thermal conductivity in porous media: Percolation-based effective-medium approximation," *Water Resources Research*, vol. 52, no. 1, pp. 295–314, 2016. [Online]. Available: <https://agupubs.onlinelibrary.wiley.com/doi/abs/10.1002/2015WR017236>
- [13] D. S. McLachlan, "The percolation exponents for electrical and thermal conductivities and the permittivity and permeability of binary composites," *Physica B: Condensed Matter*, vol. 606, p. 412658, 2021. [Online]. Available: <https://www.sciencedirect.com/science/article/pii/S0921452620306475>
- [14] S. Jadon, "Introduction to different activation functions for deep learning," *Medium, Augmenting Humanity*, vol. 16, 2018.
- [15] S. R. Dubey, S. K. Singh, and B. B. Chaudhuri, "Activation functions in deep learning: A comprehensive survey and benchmark," *Neurocomputing*, vol. 503, pp. 92–108, 2022. [Online]. Available: <https://www.sciencedirect.com/science/article/pii/S0925231222008426>